PERGAMON

Carbon 40 (2002) 1123–1130

CARBON

Scrolls and nested tubes in multiwall carbon nanotubes

J. Gerard Lavin[a], Shekhar Subramoney[a,*], Rodney S. Ruoff[b], Savas Berber[c], David Tománek[c]

[a]*Du Pont Central Research and Development, Experimental Station, Wilmington, DE 19880-0228, USA*
[b]*Department of Mechanical Engineering, Northwestern University, 2145 Sheridan Drive, Evanston, IL 60208-3111, USA*
[c]*Department of Physics and Astronomy, Michigan State University, East Lansing, MI 48824, USA*

Received 19 December 2001; accepted 18 January 2002

Abstract

Recent high-resolution transmission electron microscopy (HREM) studies of multiwalled carbon nanotubes (MWCNTs) reveal a class of defects analogous to edge dislocations in a crystal. These defects are believed to mark the transition from scrolls on one side to nested tubes on the other. On the tube side, layer spacing becomes irregular. Analysis of the helicity of the tubes shows a strong correlation between diameter and helicity. This suggests that the organizing principle for the tubes is not Van der Waals forces, as in the case of graphite or turbostratic carbon, but preservation of helicity. Based on these observations and total energy calculations, the authors speculate that graphene monolayers initially form scrolls and subsequently transform into multiwall nanotubes through the progression of defects. Scrolls and nested tubes thus coexist within a single MWNT. © 2002 Published by Elsevier Science Ltd.

Keywords: A. Carbon nanotubes; C. Transmission electron microscopy; D. Defects, Microstructure

1. Introduction

Multiwalled carbon nanotubes (MWCNTs) were discovered in 1991 by Iijima [1] in the plasma of a carbon arc used to make fullerenes, this time at pressures below 1 atm. Later, single-walled carbon nanotubes were discovered from a somewhat similar process [2]. Although the existence of MWCNTs formed by catalytic processes had been known for decades [3–5], the relatively defect-free structures of the MWCNTs formed in the extremely high temperatures of the arc-discharge process (about 5000 °C) have been intriguing enough to lead to a number of studies on their unique structure and properties [6–9].

From a historic perspective, the discovery of sub-micron size 'graphite whiskers', with a microstructure analogous to MWCNTs, was first reported by Bacon in 1960 [10]. These whiskers were made in a DC carbon arc, in inert gas at a pressure of 93 atm. By passing a large current through one of these 'whiskers' and exploding one of its ends, Bacon observed that they possessed a scroll-like microstructure. A very recent study on the cross-sectional structure of vanadium oxide nanotubes [11], albeit at significantly higher resolutions, illustrates the co-existence of scrolled and nested structures within individual tubes.

Analysis of the structure of MWCNTs processed by the arc-discharge method started with their discovery in 1991. Initially observed by high-resolution transmission electron microscopy (HREM), the MWCNTs were proposed to be made of carbon atom hexagonal sheets arranged in a helical fashion about the tube axis [1]. With the diameters of most arc-discharge produced carbon nanotubes approximately in the 10-nm range combined with their rather symmetrical microstructures, several theoretical predictions were made about their unique electronic and physical properties [12–14]. Considering how important the precise microstructure of individual nanotubes would be in dictating specific properties, characterizing the structure of these novel materials at the atomic level became a paramount issue for several researchers. Among various analytical techniques, HREM has clearly been the most applied technique for studying the intricate structure of MWCNTs in detail, providing information on how the tubes are stacked, the nature of defects, and the structure of internal as well as external closures [15]. Other analytical methods

*Corresponding author. Fax: +1-302-695-1351.
E-mail address: shekhar.subramoney@usa.dupont.com (S. Subramoney).

0008-6223/02/$ – see front matter
PII: S0008-6223(02)00050-7

have been also used for the structural characterization of MWCNTs: X-ray diffraction for crystallographic measurements [16], scanning probe microscopy for surface topography at the atomic scale [17], and electron diffraction to analyze the internal structure on a detailed basis [18].

Visual inspection of a large number of HREM images of MWCNTs clearly illustrates that these materials have a highly complex structure fraught with numerous defects. It is believed that the chaotic environment associated with evaporation of graphite electrodes in an arc leads to these complex structures. In this paper we discuss the structure of 'hybrid' MWCNTs composed of scrolled and nested segments, with the respective features typically separated from each other by defects such as edge dislocations.

2. Experimental

The MWCNTs analyzed in this work were prepared by the arc-discharge process involving dual graphitic electrodes, similar to those used by Ebbesen and Ajayan for large scale synthesis of MWCNTs [19]. The conditions inside the reaction vessel included a helium atmosphere at 500 Torr, and operating voltage and current at 20 V and 100 Amp, respectively. The gap between the anode and the cathode was maintained at ~1 mm by continuously translating the anode during the experiment with a motor. As outlined earlier by numerous researchers, the anode is consumed and a cylindrical growth occurs on the face of the cathode during the arc discharge process. The MWCNTs are found in the core of this cylindrical growth.

The MWCNT samples obtained from the core of the cathode following the arc-discharge process were dispersed using pure ethanol onto holey carbon coated transmission electron microscopy (TEM) grids. HREM was performed on a Philips CM-20 high-resolution TEM equipped with an Ultratwin polepiece. The microscope was operated at an accelerating voltage of 200 kV and images were recorded under conventional conditions on sheet films.

3. Theoretical

It is now well established that the strain energy involved in deforming an sp^2 bonded graphene sheet can be well described by continuum elasticity theory [20,21]. The key quantities in this formalism are the flexural rigidity of a graphene sheet, $D = 1.41$ eV, and Poisson's ratio $\alpha = 0.165$. The energy needed to bend a graphene monolayer into a cylinder of radius R is

$$\Delta E_s = \pi D\, L/R = \epsilon_{cyl} L/R \quad (1)$$

where $\epsilon_{cyl} = 4.43$ eV and L is the axial length. The corresponding strain energy for a spherical structure is independent of the radius, and is given by

$$\Delta E_s = 4\pi D\,(\alpha + 1) = 20.6 \text{ eV} \quad (2)$$

The interlayer interaction ΔE_I, which stabilizes multiwall structures, is proportional to the contact area A and given by

$$\Delta E_i = \epsilon_{VdW} A \quad (3)$$

where $\epsilon_{VdW} = 2.48$ eV/nm^2. The latter value, obtained from graphite, is based on an interlayer separation of 0.34 nm that is common to virtually all sp^2 bonded structures. Finally, there is an energy penalty ΔE_e associated with the generation of an exposed edge

$$\Delta E_e = \epsilon_e L \quad (4)$$

where $\epsilon_e = 21$ eV/nm is an average value for graphite [22] and L is the length of the exposed edge.

The reference system in all these considerations is a large graphene monolayer with no exposed (or completely saturated) edges. Formation of a scroll requires the energy to form two edges along the entire axis and the strain energy associated with rolling up the sheet. A scroll will be stable as long as the energy gain upon forming interwall interactions outweighs this energy investment. Formation of a multiwall nanotube involves the strain energy to form the individual cylindrical wall, which is compensated by a similar gain due to interlayer interactions. We observe that these two energies are comparable for multiwall systems with the same inner and outer radius, whether a scroll or a multiwall tube composed of nested cylinders. Since the scroll contains two edges along the entire length, it should be intrinsically less stable than a multiwall nanotube. As a transformation between these two structures involves bond rearrangement, the metastable scroll could in principle co-exist with the more stable multiwall system of nested cylinders.

4. Results and discussion

In this work, we use a kinematic approach for analyzing the HREM images of MWCNTs as a working hypothesis. Recently, using this approach, minute changes of the interwall spacing in MWNTs were investigated quantitatively [23]. In view of the level of detail in our analysis, extra caution is being paid to avoiding potential artifacts, such as mistaking interference fringes for graphitic layers. Even though complex structures, such as bent MWNTs, will produce intriguing diffraction patterns, it is inconceivable that artifacts such as a discontinuity in the number of walls would occur only in one and not the opposite wall of the same tube without a corresponding structural defect. While a dynamical analysis will probably give a more complete account of the scattering processes than a purely kinematic approach in such studies involving HREM, the associated complexity of the modeling calculation makes

this approach prohibitively involved for the nanotubes analyzed in this paper. The kinematic approach followed in this work is currently state-of-the-art for HREM studies of MWCNTs, and we expect our results to be confirmed by a dynamical interpretation in the future.

One of the most common defects observed in most of the MWCNTs studied in this work was the variation in thickness of the tube wall along the perimeter, as illustrated in Fig. 1. This TEM image shows essentially a longitudinal cross-section of this tubular system, showing a 'pair of thick walls' separated by the inner cavity. While the interlayer spacing of the (0002) graphene planes on the thinner of the two walls appears fairly uniform, the variation in interplanar spacings is fairly significant on the thicker wall. The number of independent (0002) interplanar spacings observed on the thicker wall considerably exceeds two singular spacings as suggested by Amelinckx et al. [7]. This anomaly was observed in most of the MWCNTs observed in this sample and it may be attributed to specific formation conditions that existed in the arc during the synthesis. Even though the interplanar spacing on the thinner wall appears fairly uniform on a visual basis, data generated in this work indicates that the graphene planes comprising the thinner wall exhibit a small but clearly significant variation in layer-to-layer spacing.

The classic variation in the interplanar spacing of the graphene sheets on the lower wall is indicated by the letter B in Fig. 1. Further examination of this MWCNT along its length reveals a previously undiscovered feature. It shows what appears to be a classic slip-plane defect, marked by the letter A. We believe that this defect marks the boundary between a scroll and a nested tube configuration within the same MWCNT. Interestingly enough, visual examination of this MWCNT for lengths of about 300 nm on either side of A indicated that the wall thickness was more or less uniform to the left, but the interplanar spacings on the lower wall became larger and larger on the right of point A, such as at point B.

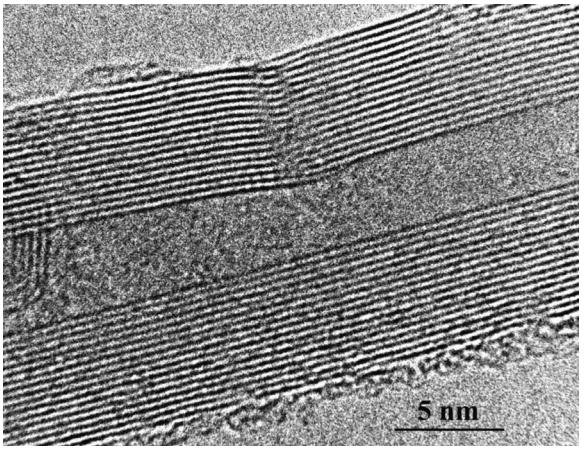

Fig. 2. Enlargement of the slip plane defect in Fig. 1, marking a junction of scroll and nested tube sections.

An enlargement of the defect (marked as A in Fig. 1) is shown in Fig. 2, and a pair of terminating (0002) lattice fringes are clearly visible in this image. This feature is associated with an edge dislocation running parallel to the axis of the MWCNT and this indicates that such an edge dislocation causes a changeover from scroll-like to a nested configuration (or vice versa) of the MWCNT. It appears that most of the MWCNTs examined in this sample flip-flopped between the scroll-like and nested structures by well-marked defects along the length of the nanotubes.

Another HREM image of a MWCNT exhibiting significant variable layer spacing in one of its walls is shown in Fig. 3. The most interesting feature of this particular tube

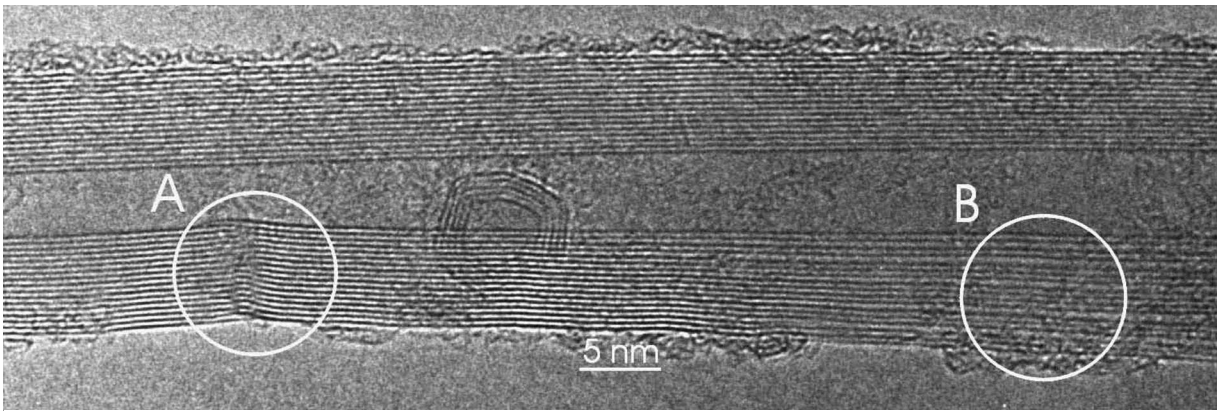

Fig. 1. Transmission electron micrograph of a multiwall carbon nanotube with a slip-plane defect and irregular layer spacing.

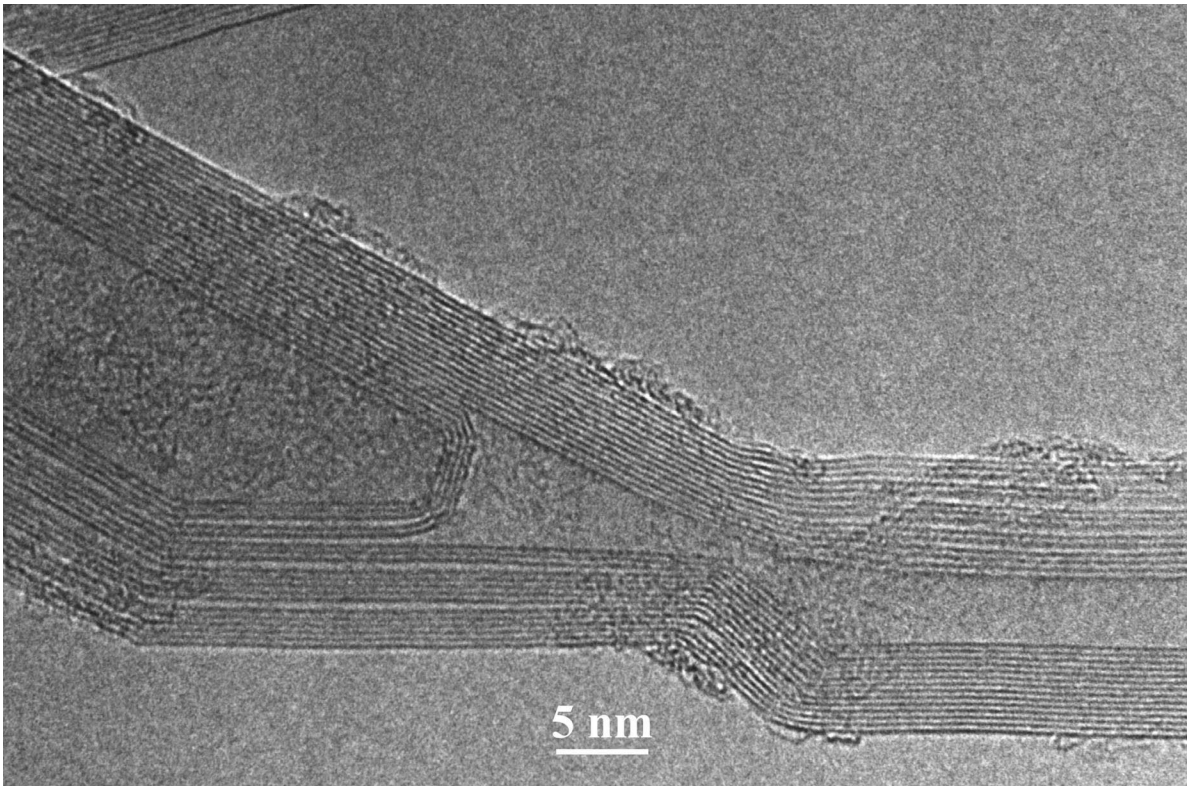

Fig. 3. Irregular layer spacing shifting from side to side and internal caps associated with irregular layer spacing.

is that a series of defect structures causes the variable layer spacing to change from one wall to the other. It appears that strategically placed lattice defects such as pentagons and heptagons can account for changing the eccentric nature of the MWCNT from one wall to the other. Analysis of several images indicates that the variable layer spacing is associated with nested eccentric tubes. Support for this belief is also observed in Fig. 3, which shows internal caps associated with variable layer spacing. The caps are inconsistent with a scroll configuration.

The defect structure that accounts for the noticeable variation in the layer spacing of the (0002) lattice fringes on one wall of the MWCNT sometimes manifests itself as an extra layer plane in the immediate vicinity of the defect site. This is clearly illustrated in the HREM image of the MWCNT shown in Fig. 4. An extra layer plane is clearly visible within the circle marked on the lower wall of the tube compared to the number of layer planes on the upper wall, which lends further credence to the co-existence of nested and scrolled structures in MWCNTs separated by defects. As observed in several other instances, a noticeable variation in the interplanar spacing is visible to the left side of the defect on the lower wall of the tube.

The mechanism responsible for variable lattice spacing was not immediately obvious. In a search for clues, nested tubes were examined for helicity utilizing image analysis via graphics software (CORELDRAW). HREM images were printed at a magnification of 1.7 million, and scanned to form digital images. Selected parts of four tubes were cropped in Corel PHOTOPAINT, and imported into CORELDRAW. This software is vector-based, and precise information is

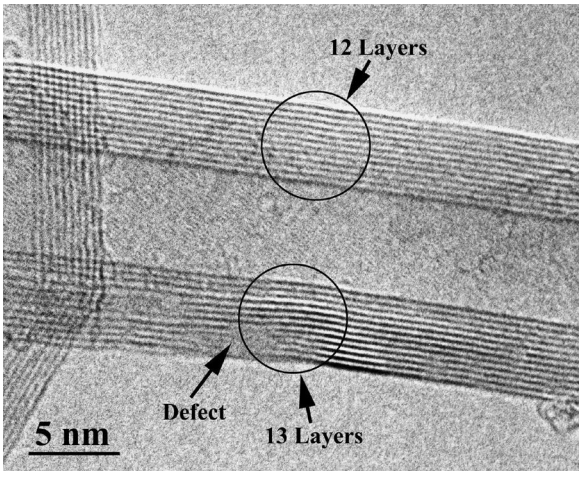

Fig. 4. Extra layer plane in the vicinity of slip-plane defect.

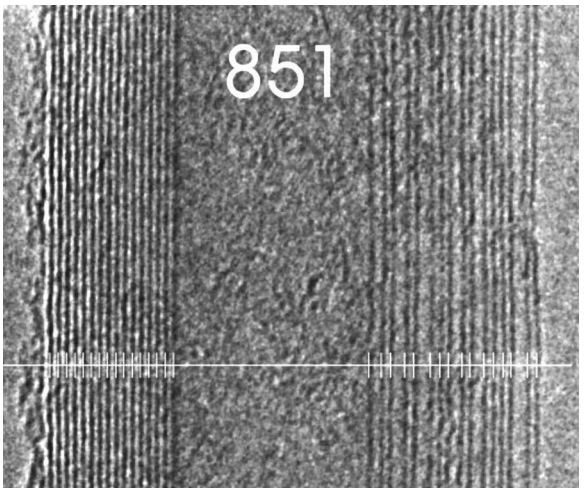

Fig. 5. Lattice spacing determination.

available on the coordinates of each line. The images were enlarged 16 or 32×, and white lines drawn in the center of the dark areas, as determined by eye (see Fig. 5). From the coordinates of the individual lines, lattice spacings and tube diameters were calculated. Minimum helicity was calculated by determining the number of repeat units (Fig. 6) contained in the tube circumference, rounded upwards to the next integer.

The helicity was calculated as the arccosine of the tube circumference divided by the number of repeat units times unit length. In this work, helicity is defined as the deviation from the armchair configuration, in contrast to the chirality defined by the conventional roll-up vector, in which the armchair configuration has an angle of 30°. The angle of the chiral vector can be determined by subtracting

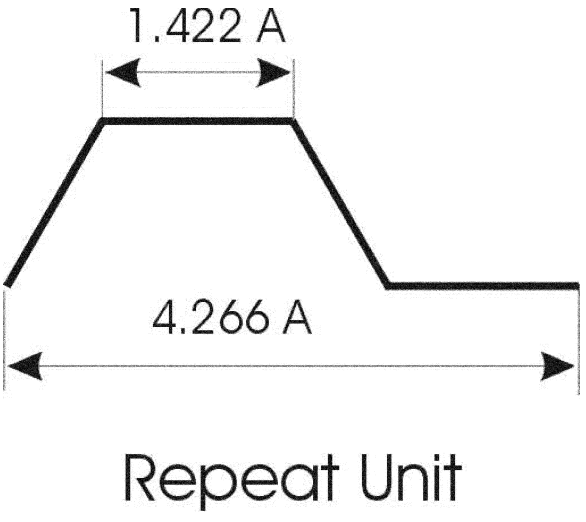

Fig. 6. Repeat unit.

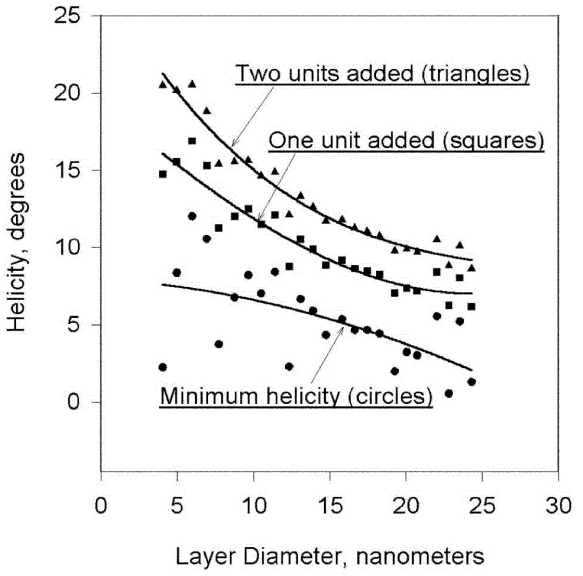

Fig. 7. Effect of excess repeat units on helicity, for nanotube from image 863.

the helicity calculated in this work from 30°. Handedness was assumed to be the same for all layers. When the minimum helicity was plotted against tube diameter, a pattern appeared of decreasing helicity with increasing diameter, but with a great deal of scatter. When an extra repeat unit was added, helicity decreased monotonically with tube diameter, and when a second repeat unit was added, scatter decreased noticeably. These data, for a single nanotube, are plotted in Fig. 7.

Lattice spacing and tube diameter data were collected on three additional tubes, of varying inside diameter and number of layers (see Table 1). Data for the four tubes, with two extra repeat units are plotted in Fig. 8. The correlation line is developed from a simple cubic equation, and the correlation coefficient is a remarkably high 0.945. The helicity of a nested tube appears to be dependent only upon its diameter! The equation for the correlation is:

Φ = helix angle, degrees: d = layer diameter, nm

$$\Phi = 29.3136 - 2.3343d + 0.1049d^2 - 0.0018d^3$$

Several observations should be made. First, a multiwall

Table 1
Characteristics of multiwall nanotubes

Tube no.	O.D. (nm)	I.D. (nm)	No. of layers
863	24.3	4.07	24
858a	15.12	3.91	14
851	22.23	8.92	16
862	18.84	5.42	17

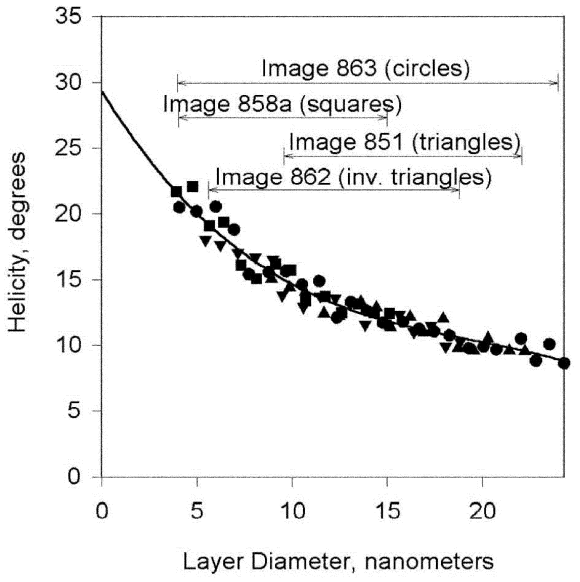

Fig. 8. Helicity vs. layer diameter, with two added repeat units.

structure is probably the lowest energy form for the nanotube, analogous to graphite heat treated at high temperatures. The rearrangements necessary at the transition between scroll and nested tube represent major defects, much more serious for nanotube strength than Stone–Wales reorganizations. Second, there is no guarantee that the nested tubes used in this analysis were imaged at their maximum diameter, although the quality of the correlation suggests that the numbers obtained are close. The simple algorithm proposed shows that a small change in helicity takes place from layer to layer, the increments being small.

The rather significant variations in (0002) interplanar spacings on one wall in MWCNTs and the possible causes for this feature are not totally novel concepts in carbon nanotube research. In the introduction to [23] Kiang et al. report average layer spacing from several workers covering the range 0.34–0.375 nm, and in their own work reported values from 0.34 to 0.39 nm, depending on diameter. Also, the co-existence of scrolled (where the helicity is conserved from layer to layer) and nested features within the same nanotube has been reported previously. High-resolution electron microscopy of ultrathin cross-sections by Dravid et al. [24] of what are believed to be MWCNTs has indicated the presence of non-terminated graphene layer planes, suggesting a localized scroll-type structure. HREM and electron diffraction studies by Liu and Cowley [25] have suggested that the tubes have a polygonized cross-section that accounts for significant variations in interplanar spacings on one wall. However, a polygonal cross-section would lead to uniformly higher-spaced planes on one wall with respect to the other, as opposed to a wall with widely varying interplanar spacings from layer to layer. The growth model as proposed by Amelinckx et al. [8,9] suggests that nested and scroll type structures would be present side by side in the lateral dimensions as well, accounting for variation in chiral angle from layer to layer as well as asymmetric (0002) lattice fringe spacings. In this paper we have shown that scrolled and nested structures can occur during the growth of a MWCNT and these features are typically separated from each other by well characterized defect structures that possibly occur due to very localized variations in the arc environment. This analysis goes hand in hand with chemical property measurements that have demonstrated the presence of regions in the tubes that are intercalatable and those that are not [10,26]. Our hypothesis is that the scroll-like features are open to intercalation and de-intercalation processes and that the nested features are not.

The energetics of the cylindrical multiwall system are discussed in Fig. 9 by plotting the required energy investment to form a scroll or a MWCNT of n nested cylinders out of a graphene strip of width W. Whereas there is only one-way to form n nested cylinders, separated by 0.34 nm, from the graphene strip, we allowed the scroll to assume its optimum geometry and readjust the inner diameter.

The system of nested cylinders behaves similar to that of nested spherical shells forming an onion [20]. Keeping the number of walls fixed while increasing W leads to a reduction of the strain energy. Beyond a critical value W_c the system gains more energy by creating an extra wall and thus increasing the interwall interaction at the cost of an

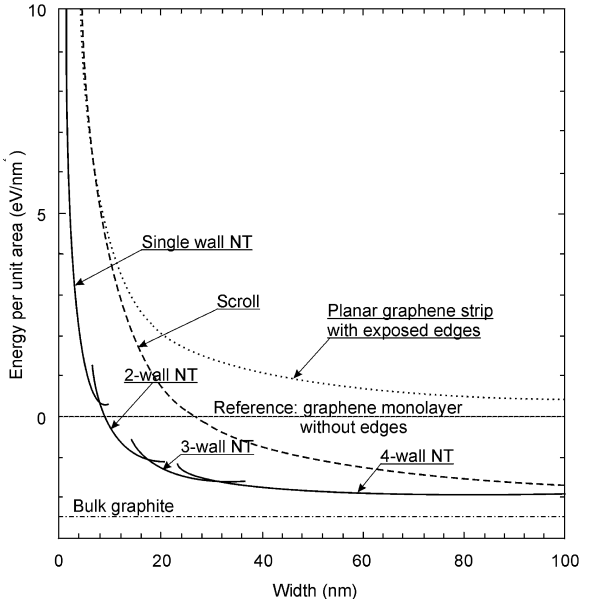

Fig. 9. Energy cost per unit area associated with the conversion of a graphene monolayer strip of width W with completely saturated edges into multiwall tubes.

increased overall strain energy. According to the results presented in Fig. 9, single-wall nanotubes are more stable only for $W < 7.7$ nm, corresponding to a tube radius of 1.2 nm. For $W > 7.7$ nm, double-wall tubes are more stable, and for $W > 17$ nm, triple-wall tubes. At each value of W, a multiwall structure consisting of nested cylinders is more stable than the optimum scroll, chiefly due to the energy penalty associated with the exposed edges. Also shown in Fig. 9 is the line denoting the relative stability with respect to a graphene strip terminated by two edges, given by $2\epsilon_e/W$. Inspection of the crossing points between this demarcation line and the energy of the individual structures indicates that for $W > 0.7$ nm, the energy gain upon eliminating two exposed edges outweighs the energy loss to form a cylinder, thus making a SWNT the preferred structure. The critical width to form a scroll is somewhat larger, with $W > 8.4$ nm. For large values of W, the energy of all multiwall structures approaches asymptotically the bulk graphite value of -2.48 eV/nm^2.

An intriguing question is, whether particular nanotubes show a preference for a conversion to a 'bamboo structure'. Let us consider a segment of a SWNT of radius R and length ΔL. If the nanotube is divided into two halves at this position, this segment is to be converted to two hemispherical domes separating and terminating the halved tubes. Since the area of the two hemispheres is $4\pi R^2$, the length of the tube segment will be $\Delta L = 4\pi R^2/2\pi R = 2R$. The strain energy stored in this segment is $2\epsilon_{cyl} = 8.9$ eV, much smaller than the energy of 20.6 eV that is needed to generate the two hemispheres. Hence, independent of the tube radius, the energy cost to subdivide a tube and close the ends by hemispherical domes is 11.7 eV.

These results suggest the following scenario for the formation of multiwall nanotubes at high temperatures. Forming graphite flakes may spontaneously roll up to form a scroll of a given helicity. During the harsh formation conditions, atomic vacancies or other defects may form that would connect the outer edge of the scroll to the neighboring wall, or any pair of adjacent walls. In this way, the topology of the scroll would be locally converted into the more stable nested cylinder structure within a MWCNT. A conversion between these structures would involve only opening and reconnecting bonds at the interface between the two structures, similar to an atomic-scale zipper. The activation energy, even though not negligible, is lower than requiring simultaneous opening of bonds along the entire length of the MWCNT. The net gain in energy upon eliminating exposed edges should drive the reaction to increase the length of the tube segments at the cost of the scroll segments.

5. Conclusions

The authors speculate that MWCNTs are complex structures composed of scroll-like and nested features existing side-by-side along their lengths, separated by well marked defects. Within the nested tubes, helicity changes little from layer to layer and depends only on layer diameter. Our proposed scenario for the formation of MWCNTs involves the formation of a scroll of a given helicity which converts, assisted by defects, into the thermodynamically more stable multiwall structure composed of nested cylinders.

Acknowledgements

The authors wish to thank Dr. Amand Lucas for useful discussions. D. Tománek, S. Berber and R.S. Ruoff were supported by the Office of Naval Research and DARPA under Grant No. N00014-99-1-0252.

References

[1] Iijima S. Helical microtubules of graphitic carbon. Nature 1991;354:56–8.
[2] Iijima S, Ichihashi T. Single-shell carbon nanotubes of 1-nm diameter. Nature 1993;363:603–5;
Bethune DS, Kiang CH, de Vries MS, Gorman G, Savoy R, Vasquez J. Cobalt-catalyzed growth of carbon nanotubes with single-atomic-layer walls. Nature 1993;363:605–7.
[3] Iley R, Riley HL. The deposition of carbon on vitreous silica, J Chem Soc 1948;Part II:1362–1366.
[4] Davis WR, Slawson RJ, Rigby GR. An unusual form of carbon. Nature 1953;171:756.
[5] Hofer LJE, Sterling E, MacCartney JT. Structure of the carbon deposited from carbon monoxide on iron, cobalt and nickel. J Phys Chem 1955;59:1153–5.
[6] Zhang XF, Zhang XB, Van Tendeloo G, Amelinckx S, Op de Beeck M, Van Landuyt J. Carbon nanotubes; their formation process and observation by electron microscopy. J Cryst Growth 1993;130:368–82.
[7] Amelinckx S, Bernaerts D, Zhang XB, Van Tendeloo G, Van Landuyt J. A structure model and growth mechanism for multishell carbon nanotubes. Science 1995;267:1334–8.
[8] Zhou O, Fleming RM, Murphy DW, Chen CH, Haddon RC, Ramirez AP, Glarum SH. Defects in carbon nanotubes. Science 1994;263:1744–7.
[9] Bretz M, Demczyk BG, Zhang L. Structural imaging of a thick-walled carbon nanotubule. J Cryst Growth 1994;141:304–9.
[10] Bacon R. Growth, structure, and properties of graphite whiskers. J Appl Phys 1960;31:283–90.
[11] Krumeich F, Muhr HJ, Niederberger M, Bieri F, Nesper R. The cross-sectional structure of vanadium oxide nanotubes studied by transmission electron microscopy and electron spectroscopic imaging. Z Anorg Allg Chem 2000;626:2208–16.
[12] Mintmire JW, Dunlap BI, White CT. Are fullerene tubes metallic? Phys Rev Lett 1992;68:631–4.
[13] Yakobson BI, Brabec CJ, Bernholc J. Nanomechanics of carbon tubes: instabilities beyond linear response. Phys Rev Lett 1996;76:2511–4.

[14] Charlier JC, Michenaud JP. Energetics of multilayered carbon tubules. Phys Rev Lett 1993;70:1858–61.
[15] Ajayan PM, Ichihashi T, Iijima S. Distribution of pentagons and shapes in carbon nano-tubes and nano-particles. Chem Phys Lett 1993;202:384–8.
[16] Reznik D, Olk CH, Neumann DA, Copley JRD. X-ray powder diffraction from carbon nanotubes and nanoparticles. Phys Rev B 1995;52:116–24.
[17] Tsang SC, de Oliviera P, Davis JJ, Green MLH, Hill HAO. The structure of the carbon nanotube and its surface topography probed by transmission electron microscopy and atomic force microscopy. Chem Phys Lett 1996;249:413–22.
[18] Zhang XB, Zhang XF, Amelinckx S, Van Tendeloo G, Van Landuyt J. The reciprocal space of carbon nanotubes: a detailed interpretation of the electron diffraction effects. Ultramicroscopy 1994;54:237–49.
[19] Ebbesen TW, Ajayan PM. Large-scale synthesis of carbon nanotubes. Nature 1992;358:220–2.
[20] Tománek D, Zhong W, Krastev E. Stability of multishell fullerenes. Phys Rev B 1993;48:15461–4.
[21] Robertson DH, Brenner DW, Mintmire JW. Energetics of nanoscale graphitic tubules. Phys Rev B 1992;45:12592–5.
[22] Thess A, Lee R, Nikolaev P, Dai H, Petit P, Robert J, Xu C, Lee YH, Kim SG, Colbert DT, Scuseria G, Tománek D, Fischer JE, Smalley RE. Crystalline ropes of metallic carbon nanotubes. Science 1996;273:483–7.
[23] Kiang CH, Endo M, Ajayan PM, Dresselhaus G, Dresselhaus MS. Size effects in carbon nanotubes. Phys Rev Lett 1998;81:1869–72.
[24] Dravid VP, Lin X, Wang Y, Wang XK, Yee A, Ketterson JB, Chang RHP. Buckytubes and derivatives: their growth and implications for buckyball formation. Science 1993;259:1601–4.
[25] Liu M, Cowley JM. Structures of the helical carbon nanotubes. Carbon 1994;32(3):393–403.
[26] Mordkovitch VZ, Baxendale M, Yoshimura S, Chang RHP. Intercalation into carbon nanotubes. Carbon 1996;34(10):1301–3.